



Expression of actively soluble antigen-binding fragment (Fab) antibody and GFP fused Fab in the cytoplasm of the engineered *Escherichia coli*

Supaluk Krittanai^{1,2} · Waraporn Putalun^{1,2} · Seiichi Sakamoto³ · Hiroyuki Tanaka⁴ · Thaweesak Juengwatanatrakul⁵ · Gorawit Yusakul^{6,7}

Received: 24 October 2019 / Accepted: 6 May 2020 / Published online: 11 May 2020
© Springer Nature B.V. 2020

Abstract

The expression of recombinant antibody fragments in the cytoplasmic space of *Escherichia coli* and the refolding process for restoring the structure and activity of such antibodies are not efficient. Herein, fragment antigen-binding (Fab) antibodies against miroestrol and deoxymiroestrol (MD-Fab) and their fusions with a green fluorescent protein (GFP) were expressed. The reactive MD-Fabs were successfully expressed as soluble and active forms in the cytoplasm of the SHuffle® T7 *E. coli* strain. Regarding the construct of MD-Fab alone, V_H-C_H1 could associate V_L-C_L into Fab in the oxidizing cytoplasm of the *E. coli* strain, and no additional in vitro refolding was needed. In the case of the fusions with GFP, when the C-terminus of V_H-C_H1 was linked with the N-terminus of GFP, the MD-Fab binding reactivity was retained, but the fluorescent activity of GFP interfered. When the C-terminus of GFP was linked to the N-terminus of V_L-C_L, the binding activity of MD-Fab was not observed. The constructed MD-Fabs had higher specificity toward deoxymiroestrol than the parental monoclonal antibody clone 12G11. In conclusion, MD-Fabs could be expressed using SHuffle® T7 *E. coli* cells. This process could be considered an economical, productive, and effective method to produce antibody fragments for immunoassay techniques.

Keywords *E. coli* · Fragment antigen binding · Deoxymiroestrol · Miroestrol · *Pueraria candollei*

Introduction

Recombinant antibody fragments expressed in the *Escherichia coli* expression system are more likely to accumulate in the cytoplasmic space where proteins are kept in reduced and inactive forms. Further treatment steps, including

denaturation and refolding, need to be implemented to restore the structure and activity of such antibodies [1]. To avoid the refolding process, recombinant proteins carrying disulfide bonds can be expressed in the periplasm because the *E. coli* periplasmic enzymes (disulfide oxidoreductases and isomerases) catalyze the proper protein folding and formation of disulfide bonds [2]. However, the periplasmic compartment is narrow, limiting the accumulation of the expressed protein [3]. Thus, *E. coli* was not the preferred choice for antibody fragment production in the past.

Electronic supplementary material The online version of this article (<https://doi.org/10.1007/s11033-020-05502-7>) contains supplementary material, which is available to authorized users.

✉ Gorawit Yusakul
gorawit.yu@wu.ac.th; gorawit.yu@mail.wu.ac.th

¹ Faculty of Pharmaceutical Sciences, Khon Kaen University, Khon Kaen 40002, Thailand

² Research Group for Pharmaceutical Activities of Natural Products Using Pharmaceutical Biotechnology (PANPB), National Research University, Khon Kaen University, Khon Kaen 40002, Thailand

³ Graduate School of Pharmaceutical Sciences, Kyushu University, Fukuoka 812-8582, Japan

⁴ Department of Pharmacognosy and Kampo, Faculty of Pharmaceutical Sciences, Sanyo-Onoda City University, 1-1-1 Daigaku-Dori, Sanyo-Onoda, Yamaguchi 756-0884, Japan

⁵ Faculty of Pharmaceutical Sciences, Ubon Ratchathani University, Ubon Ratchathani 34190, Thailand

⁶ School of Pharmacy, Walailak University, Thaiburi, Thasala, Nakhon Si Thammarat 80160, Thailand

⁷ Drug and Cosmetics Excellence Center, Walailak University, Thaiburi, Thasala, Nakhon Si Thammarat 80160, Thailand

Although eukaryotic expression systems, such as insect cells and mammalian cells, produce and secrete active antibodies efficiently, their production is expensive, and the culture is time-consuming. The SHuffle® T7 *E. coli* strain was established to achieve the correct and efficient folding of recombinant proteins within the cytoplasm [4]. This *E. coli* strain produces active protein without the need for additional refolding steps. This strain is useful in the production of nonglycosylated antibody fragments. Therefore, the production of antibody fragments in *E. coli* is an economic strategy for immunoassay development.

Immunoassays are highly sensitive and specific for phytochemical analysis because of specific lock-and-key interactions between the antibodies and epitopes of target compounds. Immunoassays resolve the chemical interferences that are the major obstacles for reliable analysis using chromatography-based HPLC-UV. Using the hybridoma technique, we generated a specific monoclonal antibody against miroestrol and deoxymiroestrol (MD-mAb) [5]. Nevertheless, the method used involves animal cell culture, which is challenging to handle and requires high maintenance costs. Previously, an alternative, relatively cheaper, and advanced technique for recombinant antibody production using an *E. coli* expression system was developed to reduce these difficulties. The *E. coli* cell system was established as a factory for producing antibody fragments against small molecules, such as plumbagin [6], ginsenosides [7], ganoderic acid A [8], wogonin glucuronide [9], and paclitaxel [10]. The *E. coli* produced these antibody fragments, and refolding steps were required. Otherwise, eukaryotic host cells were needed for the expression of the active antibody fragment. The construction of recombinant antibodies through genetic modification has widened their application, and the genetic coupling of fluorescent or other reporter proteins with the genes of the antibody fragments is possible and simple. The utilization of fluobodies (proteins fused to green fluorescent protein (GFP) combined with antibody) ranges from tracing protein localization [11], studying the cell cycle [12], and detecting gene expression [13] to fluorescence-linked immunosorbent assay (FLISA) [14].

Miroestrol and deoxymiroestrol are the most potent phytoestrogens of *Pueraria candollei* (white Kwao Krua) and have high potential as agents for relieving menopausal symptoms, including hot flashes, night sweats, mood instability, and vaginal dryness in aged women. From clinical studies with *P. candollei*, only mild side effects, such as abdominal bloating, headache, and dizziness, were reported; thus, these compounds were considered safe at specific doses [15–17]. Overconsumption of *P. candollei* can cause undesirable effects due to its high estrogenicity, and the miroestrol and deoxymiroestrol contents of *P. candollei* roots vary dramatically. For optimal consumption of effective and safe dosages, analytical methods for miroestrol and deoxymiroestrol are

necessary for potency-based quality and quantity control. Herein, the genes encoding specific fragment antigen-binding antibodies against miroestrol and deoxymiroestrol (MD-Fab) were constructed from the hybridoma clone 12G11 [5]. The pET21b(+) dual expression vector was constructed for MD-Fab expression using SHuffle® T7 *E. coli*. In addition, the GFP gene was inserted in a gene encoding light (V_L-C_L) and heavy antibody chains (V_H-C_H1) to investigate the effect of GFP orientation on Fab-binding properties. The binding characteristics of the MD-Fabs were evaluated and described in this study.

Materials and methods

Chemical and immunological reagents

The details of the chemical and immunological reagents used in this research are described in the Electronic Supplementary Material (ESM).

Construction of genes encoding anti-MD Fab and their expression vector

The nucleotide sequences of MD-Fab were cloned from the hybridoma cell clone 12G11, producing MD-mAb [5]. The methods for expression vector construction, including DNA template, PCR conditions, and primers used, were described in detail in the ESM. Briefly, cDNA was synthesized using the mRNA of the hybridoma cell. The genes encoding the V_H-C_H1 and V_L-C_L domains of MD-mAb were amplified via PCR with mixed degenerate forward primers [18] and reverse primers of C_H1 and C_L [19]. V_H-C_H1 and V_L-C_L were purified and then ligated with the pMD20-T vector. After that, the recombinant pMD20-T vectors were transformed into competent *E. coli* JM109 cells, and blue-white screening was carried out for selection. The sequences of the inserted genes were revealed using BigDye® Terminator v1.1. The CDRs of V_L-C_L and V_H-C_H1 were identified using the methods described by Kabat and Chothia (<https://www.bioinf.org.uk/abs/>). Then specific primers were designed for the construction of dual pET21b(+) vectors harboring expression cassettes for MD-Fab expression.

Using cDNA as a template, V_L-C_L was amplified and digested with BamHI/SacI. The pET21b(+) vector was also digested with the same enzymes, and then V_L-C_L was ligated with the digested pET21b(+) vector. The ligated products were introduced into competent *E. coli* JM109 cells. V_H-C_H1 was amplified and then double-digested with SalI/NotI. The pET21b(+)/ V_L-C_L was double-digested with SalI/NotI as well, and then was ligated with V_H-C_H1 and transformed into competent *E. coli* JM109 cells. Colony PCR was performed to identify recombinant

vectors of pET21b(+)/MD-Fab (Fig. 1a, cassette No. 1). Finally, recombinant pET21b(+)/MD-Fab was transformed into cells of the expression strain SHuffle® T7 *E. coli*.

Construction of the gene encoding $V_H-C_H1-(GGGS)_3$ -GFP and its expression vector

The pAcGFP1-N1 vector (Clontech, CA, USA) encoding GFP from *Aequorea coerulea* was used as the template

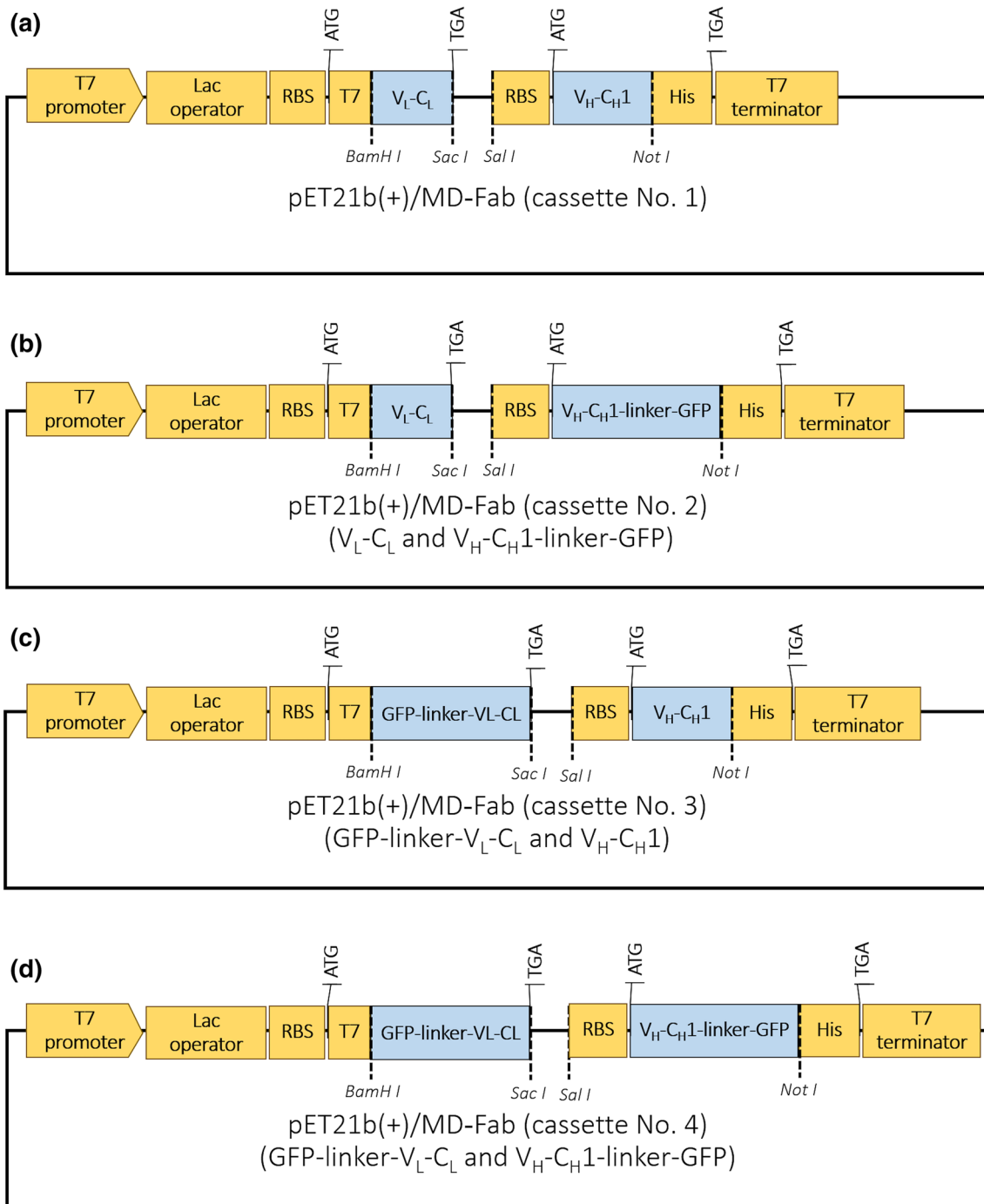


Fig. 1 Schematic diagrams of expression vectors of MD-Fab and its chimeric forms with different orientations of green fluorescent protein (GFP), including recombinant vectors of **a** pET21b(+)/MD-Fab (cassette No. 1), **b** pET21b(+)/MD-Fab [V_L-C_L and V_H-C_H1 -(GGGS)₃-

GFP] (cassette No. 2), **c** pET21b(+)/MD-Fab [GFP-(GGGS)₃- V_L-C_L and V_H-C_H1] (cassette No. 3), and **d** pET21b(+)/MD-Fab [GFP-(GGGS)₃- V_L-C_L and V_H-C_H1 -(GGGS)₃-GFP] (cassette No. 4)

for amplification of the GFP gene. The gene encoding $V_{H-C_H1}-(GGGGS)_3$ -GFP was constructed by splicing by overlap extension PCR (SOE-PCR). The PCR conditions and primers were described in the ESM. Briefly, the V_{H-C_H1} and GFP genes were amplified and then linked into the configuration $V_{H-C_H1}-(GGGGS)_3$ -GFP. Then, the resulting fragment was digested with Sall/NotI and subcloned into digested pET21b(+)/ V_L-C_L to obtain pET21b(+)/MD-Fab [V_L-C_L and $V_{H-C_H1}-(GGGGS)_3$ -GFP] (Fig. 1b, cassette No. 2). The sequences of inserted genes were confirmed, and the confirmed plasmids were transformed into SHuffle® T7 competent *E. coli*.

Construction of the gene encoding GFP-(GGGGS)₃-V_L-C_L and its expression vector

Initially, V_L-C_L and GFP were amplified using PCR, and then the gene for GFP-(GGGGS)₃- V_L-C_L was constructed using SOE-PCR. The details of the PCR conditions and primers are described in the ESM as well. The PCR product of GFP-(GGGGS)₃- V_L-C_L and the pET21b(+) vector were purified and digested with BamHI/SacI before ligation. The ligated product was introduced into competent *E. coli* JM109 cells. The obtained pET21b(+)/GFP-(GGGGS)₃- V_L-C_L vector and V_{H-C_H1} fragment were digested with Sall/NotI. The resultant plasmid pET21b(+)/MD-Fab [GFP-(GGGGS)₃- V_L-C_L and V_{H-C_H1}] (Fig. 1c, cassette No. 3), which was obtained after ligation, was transformed into competent *E. coli* JM109 cells. Finally, recombinant pET21b(+)/MD-Fab cassette No. 3 was sequenced and subsequently transformed into SHuffle® T7 competent *E. coli*.

For pET21b(+)/MD-Fab [GFP-(GGGGS)₃- V_L-C_L and $V_{H-C_H1}-(GGGGS)_3$ -GFP] (Fig. 1d, cassette No. 4), $V_{H-C_H1}-(GGGGS)_3$ -GFP, which was digested by Sall/NotI, was inserted into pET21b(+)/GFP-(GGGGS)₃- V_L-C_L . Then, the resultant ligation mixture was transformed into *E. coli* JM109 cells. Finally, the sequence of genes inserted into pET21b(+)/MD-Fab cassette No. 4 was confirmed, and the confirmed plasmid was subsequently transformed into SHuffle® T7 competent *E. coli* for expression.

Expression and purification of recombinant Fab and its fusions with GFP

SHuffle® T7 *E. coli* cells harboring the recombinant pET21b(+) vector with an expression cassette were initially cultured in Terrific Broth (TB) medium (24 g/l yeast extract, 20 g/l tryptone, 4 ml/l glycerol, 0.017 M KH₂PO₄, and 0.072 M K₂HPO₄) [20] supplemented with 100 µg/ml ampicillin at 25 °C with shaking at 120 rpm overnight. Then, for expression, the culture was transferred to 50 ml of fresh TB medium supplemented with 100 µg/ml ampicillin in a 250-ml Erlenmeyer flask. The expression was performed

with shaking at 120 rpm to limit mechanical shear and protein leakage out of the cell [21]. Although the expression of the recombinant protein by SHuffle® T7 *E. coli* could be performed at 16–37 °C, the highest yield of protein expression was obtained at 25 °C [4]. Therefore, this expression was carried out at 25 °C. When the absorbance value of the culture at 600 nm (OD₆₀₀) was equal to 0.6, IPTG was added at a final concentration of 1 mM to induce protein production. The *E. coli* cells were further cultivated under the same conditions for 14 h; then, the cell pellet was collected via centrifugation at 12,000 rpm for 20 min at 4 °C. Then, lysis buffer (20 ml; 50 mM Tris-HCl pH 8, 1 mM EDTA, and 10% (v/v) glycerol) was added to wash the cells. Then, the cell pellet was lysed by incubation for 30 min (room temperature) with 1 mg/ml lysozyme in lysis buffer (11.25 ml). Sodium chloride (NaCl) and Triton X-100 were added to final concentrations of 50 mM and 0.1% (v/v), respectively. Triton X-100 was added to disrupt and permeabilize the cell membrane. Afterward, ultrasonication was implemented to induce cell break and protein release, followed by centrifugation at 14,000 rpm for 20 min at 4 °C. The supernatant included soluble protein, whereas the pellet comprised insoluble protein or inclusion bodies. The inclusion bodies were dissolved in 2 ml of 50 mM Tris-HCl containing 8 M urea. The protein concentration was determined by the Bradford protein assay method, for which bovine serum albumin (BSA) was used as the reference standard. Sodium dodecyl sulfate–polyacrylamide gel electrophoresis (SDS-PAGE) was performed to determine the size and purity of the protein.

Preliminary screening of MD-Fabs reactivity

The reactivity of MD-Fab cassettes No. 1–4 against the target antigen was then investigated via indirect ELISA (iELISA). The iELISA processes were initiated by fixing Mi-HSA (5 µg/ml in 50 mM sodium carbonate buffer (pH 9.6), 100 µl) onto the surfaces of 96-well ELISA plates for 1 h. The method for the synthesis of Mi-HSA was described previously [22]. After the excess Mi-HSA was washed out with phosphate-buffered saline (PBS) containing 0.05% (v/v) Tween 20 (TPBS), 5% (w/v, 300 µl) skimmed milk in PBS was added to the wells to diminish nonspecific binding in the later steps. After an hour of treatment with skimmed milk, the wells were rewashed. The various concentrations of crude proteins expressed for MD-Fab cassettes 1–4 (0.001–0.5 mg/ml diluted in TPBS) were prepared. The Fabs in the crude proteins were allowed to react with Mi-HSA for 1 h. The unbound proteins were washed out, and a solution of peroxidase-conjugated anti-mouse IgG (Fab specific) antibody (1:1000 dilution in TPBS, 100 µl) was added, and the reaction was incubated for 1 h. The plate was washed. The substrate

solution [0.3 mg/ml ABTS (2,2'-azino-bis(3-ethylbenzothiazoline-6-sulfonic acid) diammonium salt) dissolved in 100 mM sodium citrate buffer, pH 4, with 0.003% H₂O₂, 100 µl] was added for colorimetric development for 15 min. The absorbance was measured at 405 nm with a microplate reader model 550 (Bio-Rad Laboratories, CA, USA). All processes were performed at 37 °C. Finally, the plot between the crude protein concentration and absorbance was established for each cassette, with which their reactivity could be compared.

Purification of Fab fragments

After screening the crude protein reactivity toward Mi-HSA, the cassette(s) that exhibited high reactivity was selected for the purification process. In this step, an immobilized metal ion affinity column (IMAC) capable of trapping C-terminal histidine tags of recombinant Fab fragments was applied for the purification of expressed Fab. The purification method was implemented according to the manufacturer's instructions. Briefly, the complete His-tag purification resin was allowed to settle in a plastic column. It was equilibrated with binding buffer [50 mM Tris-HCl pH 7.4, 500 mM NaCl, 10% (v/v) glycerol, 1% (v/v) Triton X-100, and 5 mM imidazole]. According to the instructions for His-tag purification resin, Triton X-100 (0.1–1% v/v) is recommended for reducing the nonspecific binding due to hydrophobic or ionic interactions. The soluble fraction (60 ml) of crude protein was gradually passed through the purification resin. Then, the flow-through portion was reloaded three times to ensure that the polyhistidine-tagged protein was bound entirely to the Ni-resin. The nonspecifically bound substances were eliminated by washing the column with 10 ml of binding buffer and 20 mM imidazole dissolved in binding buffer. The recombinant protein was eluted with 6 ml of the same buffer containing 200 mM imidazole. The eluted fraction was dialyzed against 20 mM Tris-HCl, pH 7.4, supplemented with 10% glycerol for 5 h three times to eliminate imidazole. After purification, the concentration of purified MD-Fabs was determined by a Bradford protein assay, and their purity and molecular mass were confirmed by using nonreducing SDS-PAGE.

SDS-PAGE was performed to evaluate the presence of MD-Fabs. The crude proteins and purified MD-Fabs were separated on a 12.5% (w/v) polyacrylamide gel and then detected by staining the gel with a Coomassie Brilliant Blue Stain Kit (Nacalai Tesque, Inc., Kyoto, Japan). To preserve the inter-chain disulfide bonds between V_H-C_H1 and V_L-C_L of Fab, the SDS-PAGE analysis was analyzed under nonreducing conditions, where the 2-mercaptoethanol was omitted in the sample preparation step for analysis.

Characterization of recombinant MD-Fab

The purified MD-Fabs were characterized to reveal their binding activities. iELISA was performed to evaluate their reactivity against Mi-HSA. Indirect competitive ELISA (icELISA) was applied to determine the reactivity of MD-Fabs toward miroestrol, deoxymiroestrol, isomiroestrol, and related isoflavonoids. The iELISA procedures were the same as those in the previous section for the preliminary screening of crude protein reactivity. Moreover, icELISA was implemented to determine the inhibitory effects (competitive) of free compounds on the binding between MD-Fab and Mi-HSA. ELISA coating and blocking steps were conducted similarly to those previously described for iELISA. The miroestrol standards were dissolved in 5% (w/v) ethanol as a free antigen and added into 96-well plates followed by the addition of MD-Fab. The plates were mixed and incubated for 1 h. After the washing step, MD-Fab bound with free miroestrol was washed out of the reaction system, since it could not bind with immobilized miroestrol (Mi-HSA). Then, a 1:1000 dilution of peroxidase (POD)-conjugated anti-mouse IgG (Fab-specific) antibody was added to bind with the MD-Fab that was occupied by immobilized miroestrol. The wells were washed after 1 h of incubation. Finally, the ABTS substrate solution was added to the wells, and the color changed with respect to the available POD. Then, the absorbance of the product was measured at 405 nm using a microplate reader. The concentrations of the compounds on the logarithm scale were then plotted against the ratio of A/A₀, where A₀ is the absorbance in the absence of any compound, and A is the absorbance in the presence of the free compound of interest at a concentration.

The concentration that produced a 50% inhibitory effect (IC₅₀, A/A₀=0.5) was calculated from the logarithm equation of the graph. The binding specificity of the MD-Fabs antibody against compounds, including deoxymiroestrol, miroestrol, isomiroestrol, puerarin, daidzein, genistein, and kwakhurin, was determined. The icELISA was performed as previously described, and various concentrations of these free compounds were used as free antigens. Then, the relative binding properties of MD-Fab against different compounds of interest were compared, the cross-reactivity was calculated as follows:

$$\text{Cross-reactivity (\%)} = \frac{\text{IC}_{50} \text{ of deoxymiroestrol}}{\text{IC}_{50} \text{ of the assayed substance}} \times 100$$

Measurement of fluorescence intensity

The fluorescent activity of GFP was measured with EVOSTTM FL Auto 2 (Thermo Fisher Scientific Inc., UK). The

fluorescent intensity of MD-Fab cassette No. 2 was measured at 490 nm excitation and 530 nm emission wavelengths. In the experiment, the sample solution (70 $\mu\text{g}/\text{ml}$, 100 μl /well) was added to a black microtiter plate (FluoroNunc, MaxiSorp), and then fluorescence intensity was recorded.

Results and discussion

Construction of genes encoding MD-Fab and their expression vector

The genes encoding the $V_{\text{H}}\text{-C}_{\text{H}1}$ and $V_{\text{L}}\text{-C}_{\text{L}}$ regions of MD-mAb (clone 12G11) were successfully constructed, and then the sequences were registered to the Bioinformatics and DDBJ Center (accession No. LC456788 and LC456789). The lengths of $V_{\text{H}}\text{-C}_{\text{H}1}$ (IgG1) and $V_{\text{L}}\text{-C}_{\text{L}}$ (kappa) were 224 and 219 amino acids, respectively. The complete amino acid sequences and CDRs of these genes are shown in Fig. S1 of the ESM. When the sequences of V_{H} and V_{L} were compared with those of highly specific scFv toward miroestrol [23], the sequences showed similarities of 36 and 44%, respectively. The CDRs of both domains were completely different, which corresponds to the different binding specificity.

Expression of MD-Fab in SHuffle® T7 *E. coli*

The clones of SHuffle® T7 *E. coli* occupying the recombinant vector of every cassette were cultured in TB, and then the protein was expressed using the same culturing conditions. The cell pellets were collected and lysed to obtain the soluble fraction as crude protein. The binding reactivity of crude protein containing MD-Fab was evaluated by iELISA. The binding manner was correlated with the applied concentration of crude proteins. When compared with the four expression cassettes, cassette No. 1 exhibited the highest activity, followed by cassette No. 2. However, cassettes No. 3 and 4 showed very low activity (Fig. 2). Therefore, fusing GFP to the MD-Fab genes may affect the expression or binding of MD-Fabs. A previous study also reported the effect of GFP on the secondary structure folding step, where different protein fusions (N-terminal or C-terminal) may result in different protein conformations and functions [24]. Previously, the GFP fusion with $V_{\text{L}}\text{-C}_{\text{L}}$ in both the C- and N-termini individually produced soluble forms of Fab in *E. coli*; moreover, the GFP fusions were more reactive against the target c-Met than Fab with GFP at the C-terminus heavy chain [25]. The amino acid sequence of the IgG light chain is more likely to be folded than that of the heavy chain [26]. The light chain of anti-c-Met Fab tagged with GFP in the C-terminus is more reactive than the light chain tagged with GFP in the N-terminus, where it is adjacent to the variable region [25]. The study utilized the amino acid linker

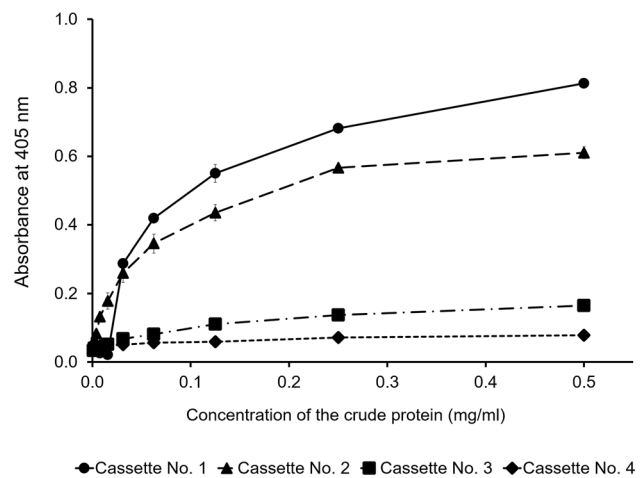


Fig. 2 Comparative reactivity of crude proteins derived from various expression cassettes, the reactivity was investigated by iELISA using Mi-HSA as an antigen

(SSGGGGSGGGGGSSRSS) between GFP and $V_{\text{H}}\text{-C}_{\text{H}}$ or $V_{\text{L}}\text{-C}_{\text{L}}$ [25], and the previously studied amino acid linker may be more flexible than the amino acid linker used in the current work. The inappropriate amino acid sequence used as a linker in this experiment may interfere with the binding of the light chain. The flexibility of the linker influences the structure and function of the protein with which GFP is linked [27]. Regarding GFP tagged at the N-terminus of $V_{\text{L}}\text{-C}_{\text{L}}$, due to the low reactivity of cassettes No. 3 and 4, these cassettes were inapplicable for further characterization. Therefore, only expressed cassettes No. 1 and 2 were selected for purification and additional characterization.

The yield of MD-Fab and purity of the protein

MD-Fab cassettes No. 1 and 2 were purified from crude protein using the IMAC column, and the protein yield was calculated according to protein concentration analyzed by a Bradford protein assay and cell density at the time of harvesting. The yields of purified MD-Fab from cassettes No. 1 and 2 were 6.0 and 2.8 mg of Fab per liter per 1.0 OD_{600} (Fab/ OD_{600}), respectively. The yield was higher than the cytoplasmic expression of Fab (0.8 mg Fab/ OD_{600}) in redox-engineered *E. coli* [28]. The size of the purified protein was estimated by SDS-PAGE (Fig. 3). The size of purified MD-Fab cassette No. 1 correlated with its theoretical molecular weight of 48.26 kDa. The GFP protein has a reported molecular weight of approximately 26.9 kDa; thus, the appearance based on SDS-PAGE analysis corresponded to the theoretical molecular weight of 75.16 kDa of MD-Fab cassette No. 2. The nonreducing SDS-PAGE (Fig. 3a) indicated that MD-Fabs were well expressed in the cytoplasm of the SHuffle® T7 *E. coli* strain. $V_{\text{H}}\text{-C}_{\text{H}1}$ and $V_{\text{L}}\text{-C}_{\text{L}}$ were expressed and assembled into the Fab structure (black

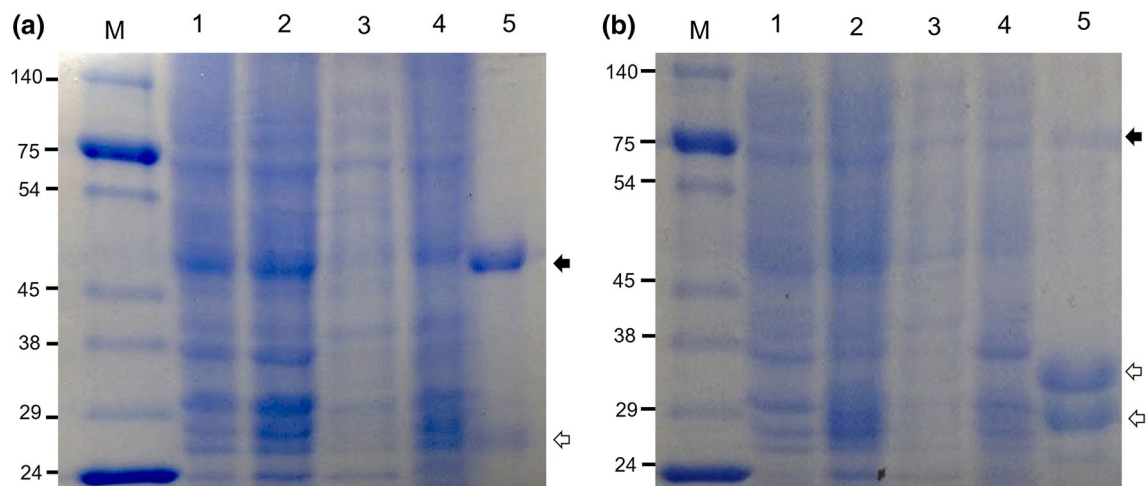


Fig. 3 SDS-PAGE (non-reducing condition) demonstrates the protein size and purity (indicated by arrow) of cassettes no. 1 **(a)** and cassettes No. 2 **(b)**. Lane M contains a protein molecular weight marker, while lanes 1, 2, 3, 4, and 5 represent cellular proteins before IPTG

induction, cellular proteins after IPTG induction, the soluble fraction (20 $\mu\text{g}/\text{well}$), inclusion bodies, and purified MD-Fab (20 $\mu\text{g}/\text{well}$), respectively

arrow); however, a small portion of $V_{\text{H}}\text{-C}_{\text{H}}1$ remained in the free domain (Fig. 3a, transparent arrow). As indicated in Fig. 3b, although MD-Fab cassette No. 2 was observed with the band with a molecular size of 75 kDa (black arrow), the amount was small. The major proteins were observed with molecular weights of approximately 27–34 kDa (transparent arrows). Both bands of protein were expected to be $V_{\text{H}}\text{-C}_{\text{H}}1\text{-(GGGS)}_3\text{-GFP}$ domains. Even if the domain was 51.9 kDa, the domain migrated faster than usual (in nonreducing SDS-PAGE) due to its secondary structures. In addition, SDS-PAGE revealed two large bands for the $V_{\text{H}}\text{-C}_{\text{H}}1\text{-(GGGS)}_3\text{-GFP}$ domain, implying that the domain folded into two conformations. For regular expression using conventional *E. coli*, the Fab domains of $V_{\text{H}}\text{-C}_{\text{H}}1$ and $V_{\text{L}}\text{-C}_{\text{L}}$ were expressed separately in reduced form in the *E. coli* cytoplasm. The structure of Fab can be recovered using in vitro refolding. The method uses chemically mediated folding, which is inefficient and inconsistent. The factors influencing the yield of recombinant protein expression in SHuffle® are medium, inducer concentration, induction temperature, and dissolved oxygen. Therefore, if these factors are strictly controlled, the expression level should be reproducible. The activity of human tissue plasminogen activator (vtPA) expressed in SHuffle® T7 grown at a specific temperature, growth phase, and IPTG condition was not largely varied during two batches of shake flask expression [4]. Thus, the expression yield of recombinant protein should be reproducible. The SHuffle® T7 *E. coli* strain was developed with an oxidizing cytoplasm, wherein disulfide bonds of both intra- and inter-domains of Fab can be formed. Previously, scFv [8] and immunoglobulin G (IgG) [29] were successfully produced using this engineered SHuffle® T7 *E. coli* strain. This

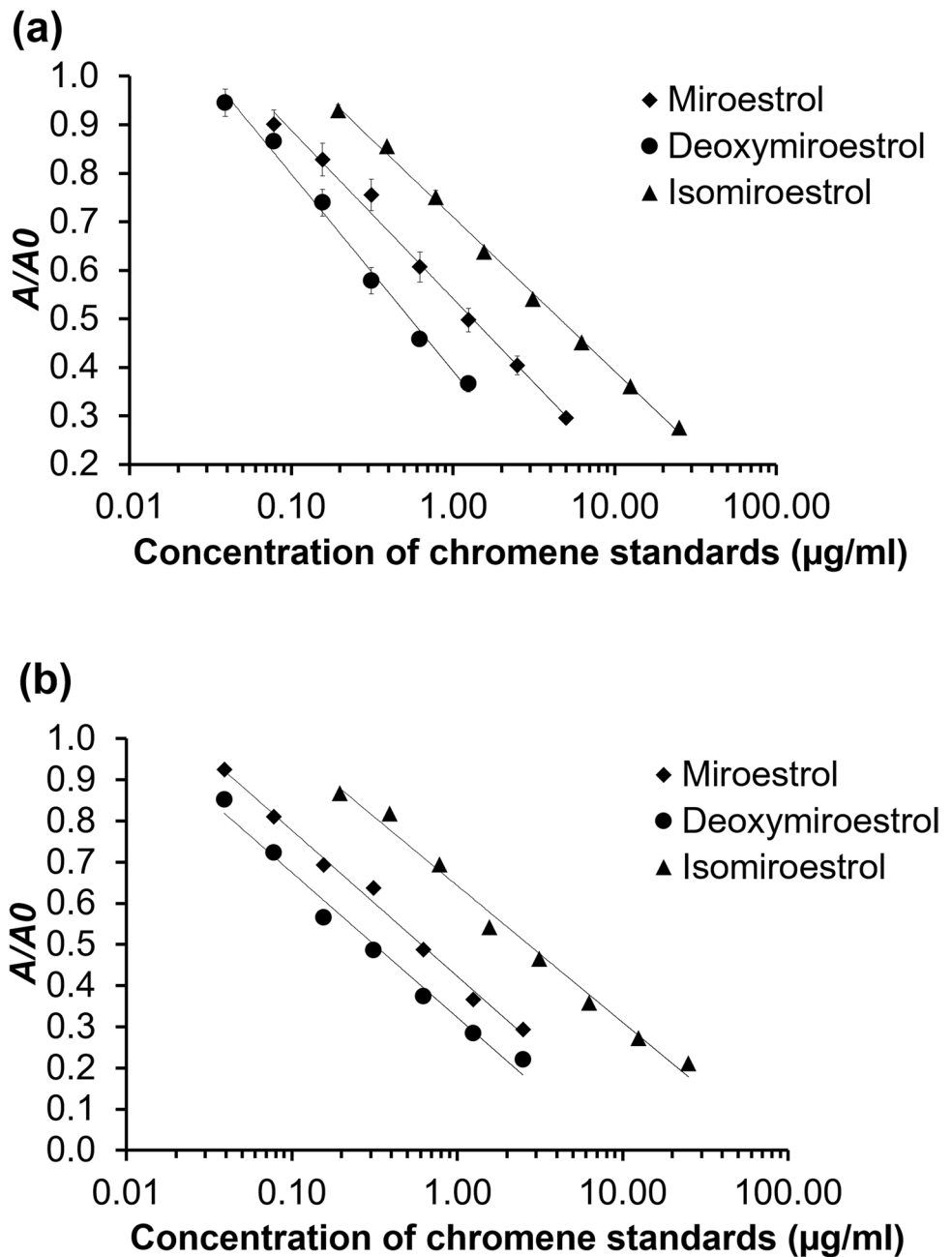
research indicated that Fab could be expressed in active form using the SHuffle® T7 *E. coli* strain. $V_{\text{H}}\text{-C}_{\text{H}}1$ can associate with $V_{\text{L}}\text{-C}_{\text{L}}$ in the structure of Fab (Fig. 3). Therefore, the expression system is useful for Fab antibody expression.

According to the fluorescent characteristics of GFP from *A. coerulescens* (Vector Information, Clontech, CA, USA), the fluorescence intensity was observed at 490 nm excitation and 530 nm emission wavelengths. The fluorescent activity of MD-Fab cassette No. 2 was not found. Previously, the single-domain antibody (scFv) toward plumbagin was fused to the N-terminus of GFP; the fluorescent activity interfered, as well. However, GFP fluorescent activity was retained when the scFv was fused to the C-terminus of GFP [30], where the peptide linker with the sequence $(\text{GGGS})_2$ was used. Thus, the linker of MD-Fab cassette No. 2 may not provide enough flexibility to avoid steric hindrance and folding interference of GFP from the $V_{\text{H}}\text{-C}_{\text{H}}1$ domain [30].

Determination of the binding specificity of the purified protein

The sensitivity and specificity of purified MD-Fab cassettes No. 1 and 2 were revealed. The icELISA was performed. The results of the icELISA are demonstrated in Fig. 4. The competitive effects of chromene groups were plotted. Cassettes No. 1 and 2 showed similar trends, indicating that purified protein has a high preference for deoxymiroestrol. MD-Fab cassette No. 1 could bind with deoxymiroestrol linearly in the concentration range of 0.039–1.25 $\mu\text{g}/\text{ml}$ ($R^2 = 0.9919$). MD-Fab cassette No. 1 reacted with miroestrol and isomiroestrol linearly in the binding ranges of 0.078–5 $\mu\text{g}/\text{ml}$ ($\text{IC}_{50} = 3.68 \mu\text{M}$, $R^2 = 0.9927$) and 0.2–25 $\mu\text{g}/$

Fig. 4 Reactivity of MD-Fabs cassettes No. 1 (a) and cassette No. 2 (b) toward deoxymiroestrol, miroestrol, and isomiroestrol, the binding reactivity was determined via indirect competitive ELISA. A/A_0 , which A_0 and A were the absorbance values in the absence and presence of the assayed substance, respectively, were plotted against the concentrations of the substance



ml ($IC_{50} = 13.56 \mu\text{M}$, $R^2 = 0.9886$), respectively. Therefore, protein from cassette No. 1 had the highest reactivity toward deoxymiroestrol ($IC_{50} = 0.54 \mu\text{g/ml}$ or $1.58 \mu\text{M}$), which was set as 100% cross-reactivity. MD-Fab cassette No. 1 showed less than 0.01% of cross-reactivity toward isoflavonoids of *P. candollei* (Table 1).

The results for MD-Fab cassette No. 2 showed a similar trend to cassette No. 1. Cassette No. 2 reacted with deoxymiroestrol in a linear manner at concentrations from 0.02 to $2.5 \mu\text{g/ml}$ ($R^2 = 0.9886$). In addition, miroestrol and isomiroestrol exhibited a competitive effect in a linear manner within the concentration ranges of 0.02– $2.5 \mu\text{g/}$

ml ($IC_{50} = 1.90 \mu\text{M}$, $R^2 = 0.9935$) and 0.2– $25 \mu\text{g/ml}$ ($IC_{50} = 7.50 \mu\text{M}$, $R^2 = 0.9886$), respectively. The IC_{50} value of deoxymiroestrol was $0.31 \mu\text{g/ml}$ ($0.905 \mu\text{M}$), which was set at 100% cross-reactivity. MD-Fab cassette No. 2 showed less than 0.01% cross-reactivity toward isoflavonoids (Table 1). Therefore, the GFP fusion on the C-terminus of $V_H\text{-}C_H1$ did not influence the binding specificity of MD-Fab. Regarding the previous report of the MD-mAb [5], deoxymiroestrol, miroestrol, and isomiroestrol exhibited an inhibitory effect in a linear manner within the concentration ranges of 15.6– 500 ng/ml ($IC_{50} = 71.2 \text{ ng/ml}$ or $0.208 \mu\text{M}$), 15.6– 500 ng/ml ($IC_{50} = 87.2 \text{ ng/ml}$ or

Table 1 Comparative cross-reactivity (%) of different forms of MD-Fabs and their parental mAb

Compound	Cross-reactivity (%)		
	MD-mAb	MD-Fab (Cassette No. 1)	MD-Fab (Cassette No. 2)
Deoxymiroestrol	100	100	100
Miroestrol	81.6	40.9	45.6
Isomiroestrol	12.3	11.1	11.5
Puerarin	0.080	<0.010	<0.010
Genistein	0.170	<0.010	<0.010
Daidzein	0.640	<0.010	<0.010
Kwakhurin	0.040	<0.010	<0.010

0.243 μM), and 0.125–4.0 $\mu\text{g/ml}$ ($\text{IC}_{50} = 0.578 \mu\text{g/ml}$ or 1.61 μM), respectively. The binding specificities of MD-Fab cassette No. 1 and Cassette No. 2 were compared with that of the parent MD-mAb clone 12G11 reported previously [5], and the Fab construct exhibited higher specificity toward deoxymiroestrol. On the other hand, the CR against miroestrol was decreased. A slight reduction in CR toward isomiroestrol was also observed. The full-length antibody (MD-mAb) consists of two binding sites for ligands, while MD-Fab has only one. This is one reason for the differences in binding specificity (Table 1). Moreover, the MD-mAb was produced by mouse hybridoma cells, and posttranslational modifications might affect the structure and binding properties of MD-mAb. These posttranslational modifications include disulfide bond formation, N-glycosylation, N-terminal pyroglutamine cyclization, C-terminal lysine processing, deamidation, isomerization, cysteinylolation, and oxidation [31]. The isomerization of Asp residues in CDRs influences the affinity of antigen binding [32–34], in which the Asp residues were found in the heavy chain CDR-2 and -3 of the MD-Fab (Fig. S1, ESM). While MD-Fabs were produced by *E. coli* cells, the processes of posttranslational modifications are different from those of hybridoma cells. Only several modifications, such as protein acetylation and phosphorylation, were reported in *E. coli* [35]. This different process is another reason for the different binding specificity between MD-Fabs and their parental MD-mAb. Because the recombinant MD-Fabs were expressed from a unique set of genes, posttranslational modification of *E. coli* was less frequent. This leads to less batch-to-batch variability of binding specificity than hybridoma-produced mAbs. With respect to stability, the previous study indicated that the stability of IgG produced in SHuffle® T7 *E. coli* was comparable to those produced by mammalian cells [3] because the *E. coli* strain mediated formation of disulfide bonds, which are essential for correct folding and stability of the expressed protein [4]. Because the binding character of MD-Fab is more specific against deoxymiroestrol, MD-Fab is promising

as a new agent for deoxymiroestrol determination. Currently, the production of anti-deoxymiroestrol mAb is not yet successful. This method could be developed as an analytical method for deoxymiroestrol.

In this study, the genes encoding MD-Fab were constructed from hybridoma cells secreting MD-mAb. GFP was genetically inserted into the sequence of MD-Fab and then subcloned into the pET21b(+) vector. The SHuffle® T7 *E. coli* was applicable for the expression of the active form of MD-Fab. The insertion of the GFP gene into the C-terminus of $V_{\text{H}}\text{-C}_{\text{H}}1$ did not attenuate antibody activity compared to other positions; however, the fluorescent intensity was not observed. Therefore, MD-Fab cassette No. 1 is appropriate for further development as an analytical reagent for immunoassays. Compared to MD-mAb, the developed Fab was more specific toward deoxymiroestrol than miroestrol. Therefore, this *E. coli* expression system is suitable for MD-Fab production. MD-Fab exhibits a high potential to be developed and validated as an analytical method for deoxymiroestrol determination.

Acknowledgements The authors would like to express gratitude to Dr. Chaiyo Chaichantipyuth, Faculty of Pharmaceutical Sciences, Chulalongkorn University, Thailand, for authentic standards.

Funding This research was supported by the Faculty of Pharmaceutical Sciences, Graduate School of Khon Kaen University, Thailand (Grant Number 590H11), and the National Research Council of Thailand (NRCT). This research was partially supported by the new strategic research (P2P) project, Walailak University, Thailand.

Compliance with ethical standards

Conflict of interest The authors declare they have no conflict of interest.

Research involving human participants and/or animals There is no research involving human participants and animals.

References

1. Frenzel A, Hust M, Schirrmann T (2013) Expression of recombinant antibodies. *Front Immunol* 4:217. <https://doi.org/10.3389/fimmu.2013.00217>
2. Sockolosky JT, Szoka FC (2013) Periplasmic production via the pET expression system of soluble, bioactive human growth hormone. *Protein Expres Purif* 87(2):129–135. <https://doi.org/10.1016/j.pep.2012.11.002>
3. Robinson MP, Ke N, Lobstein J, Peterson C, Szkodny A, Mansell TJ, Tuckey C, Riggs PD, Colussi PA, Noren CJ, Taron CH, DeLisa MP, Berkmen M (2015) Efficient expression of full-length antibodies in the cytoplasm of engineered bacteria. *Nat Commun* 6(1):8072. <https://doi.org/10.1038/ncomms9072>
4. Lobstein J, Emrich CA, Jeans C, Faulkner M, Riggs P, Berkmen M (2012) SHuffle, a novel *Escherichia coli* protein expression strain capable of correctly folding disulfide bonded

- proteins in its cytoplasm. *Microb Cell Fact* 11:56. <https://doi.org/10.1186/1475-2859-11-56>
5. Yusakul G, Kitisripanya T, Juengwatanatrakul T, Sakamoto S, Tanaka H, Putalun W (2018) Enzyme linked immunosorbent assay for total potent estrogenic miroestrol and deoxymiroestrol of *Pueraria candollei*, a Thai herb for menopause remedy. *J Nat Med* 72(3):641–650. <https://doi.org/10.1007/s11418-018-1194-x>
 6. Sakamoto S, Taura F, Putalun W, Pongkitwitoon B, Tsuchihashi R, Morimoto S, Kinjo J, Shoyama Y, Tanaka H (2009) Construction and expression of specificity-improved single-chain variable fragments against the bioactive naphthoquinone, plumbagin. *Biol Pharm Bull* 32(3):434–439. <https://doi.org/10.1248/bpb.32.434>
 7. Pongkitwitoon B, Sakamoto S, Morinaga O, Juengwatanatrakul T, Shoyama Y, Tanaka H, Morimoto S (2011) Single-chain variable fragment antibody against ginsenoside Re as an effective tool for the determination of ginsenosides in various ginsengs. *J Nat Med* 65(1):24–30. <https://doi.org/10.1007/s11418-010-0446-1>
 8. Yusakul G, Nuntawong P, Sakamoto S, Ratnatilaka Na Bhuket P, Kohno T, Kikkawa N, Rojsitthasak P, Shimizu K, Tanaka H, Morimoto S (2017) Bacterial expression of a single-chain variable fragment (scFv) antibody against ganoderic acid A: a cost-effective approach for quantitative analysis using the scFv-based enzyme-linked immunosorbent assay. *Biol Pharm Bull* 40(10):1767–1774. <https://doi.org/10.1248/bpb.b17-00531>
 9. Paudel MK, Sakamoto S, Van Huy L, Tanaka H, Miyamoto T, Morimoto S (2017) The effect of varying the peptide linker length in a single chain variable fragment antibody against wogonin glucuronide. *J Biotechnol* 251:47–52. <https://doi.org/10.1016/j.jbiotec.2017.04.002>
 10. Yusakul G, Sakamoto S, Nuntawong P, Tanaka H, Morimoto S (2018) Different expression systems resulted in varied binding properties of anti-paclitaxel single-chain variable fragment antibody clone 1C2. *J Nat Med* 72(1):310–316. <https://doi.org/10.1007/s11418-017-1136-z>
 11. Huang D, Shusta EV (2006) A yeast platform for the production of single-chain antibody-green fluorescent protein fusions. *Appl Environ Microbiol* 72(12):7748–7759. <https://doi.org/10.1128/AEM.01403-06>
 12. Niemantsverdriet M, Backendorf C (2008) TwinGFP, a marker for cell cycle analysis in transiently transfected cells. *Anal Biochem* 375(2):173–178. <https://doi.org/10.1016/j.ab.2008.01.015>
 13. Richards HA, Halfhill MD, Millwood RJ, Stewart CN Jr (2003) Quantitative GFP fluorescence as an indicator of recombinant protein synthesis in transgenic plants. *Plant Cell Rep* 22(2):117–121. <https://doi.org/10.1007/s00299-003-0638-1>
 14. Jeong GM, Kim YS, Jeong KJ (2014) A human kringle domain-based fluorescence-linked immunosorbent assay system. *Anal Biochem* 451:63–68. <https://doi.org/10.1016/j.ab.2014.01.019>
 15. Chandeying V, Lamlerkittikul S (2007) Challenges in the conduct of Thai herbal scientific study: efficacy and safety of phytoestrogen, *Pueraria mirifica* (Kwao Keur Kao), phase I, in the alleviation of climacteric symptoms in perimenopausal women. *J Med Assoc Thai* 90(7):1274–1280
 16. Manonai J, Chittacharoen A, Theppisai U, Theppisai H (2007) Effect of *Pueraria mirifica* on vaginal health. *Menopause* 14(5):919–924. <https://doi.org/10.1097/gme.0b013e3180399486>
 17. Okamura S, Sawada Y, Satoh T, Sakamoto H, Saito Y, Sumino H, Takizawa T, Kogure T, Chaichantipyuth C, Higuchi Y, Ishikawa T, Sakamaki T (2008) *Pueraria mirifica* phytoestrogens improve dyslipidemia in postmenopausal women probably by activating estrogen receptor subtypes. *Tohoku J Exp Med* 216(4):341–351. <https://doi.org/10.1620/tjem.216.341>
 18. Krebber A, Bornhauser S, Burmester J, Honegger A, Willuda J, Bosshard HR, Pluckthun A (1997) Reliable cloning of functional antibody variable domains from hybridomas and spleen cell repertoires employing a reengineered phage display system. *J Immunol Methods* 201(1):35–55. [https://doi.org/10.1016/s0022-1759\(96\)00208-6](https://doi.org/10.1016/s0022-1759(96)00208-6)
 19. Engberg J, Jensen LB, Yenidunya AF, Brandt K, Riise E (2001) Phage-display libraries of murine antibody Fab fragments. In: Kontermann R, Dübel S (eds) *Antibody engineering*. Springer, Berlin, pp 65–92
 20. Kram KE, Finkel SE (2015) Rich medium composition affects *Escherichia coli* survival, glycation, and mutation frequency during long-term batch culture. *Appl Environ Microbiol* 81(13):4442–4450. <https://doi.org/10.1128/AEM.00722-15>
 21. Chan CE, Lim AP, Chan AH, MacAry PA, Hanson BJ (2010) Optimized expression of full-length IgG1 antibody in a common *E. coli* strain. *PLoS ONE* 5(4):e10261. <https://doi.org/10.1371/journal.pone.0010261>
 22. Krittanai S, Kitisripanya T, Udomsin O, Tanaka H, Sakamoto S, Juengwatanatrakul T, Putalun W (2018) Development of a colloidal gold nanoparticle-based immunochromatographic strip for the one-step detection of miroestrol and puerarin. *Biomed Chromatogr* 32(11):e4330. <https://doi.org/10.1002/bmc.4330>
 23. Pongkitwitoon B, Boonsongcheep P, Kitisripanya T, Yusakul G, Sakamoto S, Tanaka H, Morimoto S, Putalun W (2019) Preparation of a highly specific single chain variable fragment antibody targeting miroestrol and its application in quality control of *Pueraria candollei* by enzyme-linked immunosorbent assay. *Phytochem Anal* 30(6):600–608. <https://doi.org/10.1002/pca.2832>
 24. Jansen EJ, van Bakel NH, Olde Loohuis NF, Hafmans TG, Arentsen T, Coenen AJ, Scheenen WJ, Martens GJ (2012) Identification of domains within the V-ATPase accessory subunit Ac45 involved in V-ATPase transport and Ca²⁺-dependent exocytosis. *J Biol Chem* 287(33):27537–27546. <https://doi.org/10.1074/jbc.M112.356105>
 25. Yi KS, Chung J, Park KH, Kim K, Im SY, Choi CY, Im MJ, Kim UH (2004) Expression system for enhanced green fluorescence protein conjugated recombinant antibody fragment. *Hybrid Hybridomics* 23(5):279–286. <https://doi.org/10.1089/hyb.2004.23.279>
 26. Yusakul G, Sakamoto S, Tanaka H, Morimoto S (2018) Improvement of heavy and light chain assembly by modification of heavy chain constant region 1 (CH1): application for the construction of an anti-paclitaxel fragment antigen-binding (Fab) antibody. *J Biotechnol* 288:41–47. <https://doi.org/10.1016/j.jbiotec.2018.10.009>
 27. Huang Z, Li G, Zhang C, Xing XH (2016) A study on the effects of linker flexibility on acid phosphatase PhoC-GFP fusion protein using a novel linker library. *Enzyme Microb Technol* 83:1–6. <https://doi.org/10.1016/j.enzmictec.2015.11.002>
 28. Levy R, Weiss R, Chen G, Iverson BL, Georgiou G (2001) Production of correctly folded Fab antibody fragment in the cytoplasm of *Escherichia coli* trxB gor mutants via the coexpression of molecular chaperones. *Protein Expr Purif* 23(2):338–347. <https://doi.org/10.1006/prep.2001.1520>
 29. Robinson MP, Ke N, Lobstein J, Peterson C, Szkodny A, Mansell TJ, Tuckey C, Riggs PD, Colussi PA, Noren CJ, Taron CH, DeLisa MP, Berkmen M (2015) Efficient expression of full-length antibodies in the cytoplasm of engineered bacteria. *Nat Commun* 6:8072. <https://doi.org/10.1038/ncomms9072>
 30. Sakamoto S, Pongkitwitoon B, Nakahara H, Shibata O, Shoyama Y, Tanaka H, Morimoto S (2012) Fluobodies against bioactive natural products and their application in fluorescence-linked immunosorbent assay. *Antibodies* 1(2):239–258
 31. Liu H, Gaza-Bulsecu G, Faldu D, Chumsae C, Sun J (2008) Heterogeneity of monoclonal antibodies. *J Pharm Sci* 97(7):2426–2447. <https://doi.org/10.1002/jps.21180>
 32. Cacia J, Keck R, Presta LG, Frenz J (1996) Isomerization of an aspartic acid residue in the complementarity-determining regions of a recombinant antibody to human IgE: identification and effect on binding affinity. *Biochemistry* 35(6):1897–1903. <https://doi.org/10.1021/bi951526c>

33. Rehder DS, Chelius D, McAuley A, Dillon TM, Xiao G, Crouse-Zeineddini J, Vardanyan L, Perico N, Mukku V, Brems DN, Matsumura M, Bondarenko PV (2008) Isomerization of a single aspartyl residue of anti-epidermal growth factor receptor immunoglobulin gamma2 antibody highlights the role avidity plays in antibody activity. *Biochemistry* 47(8):2518–2530. <https://doi.org/10.1021/bi7018223>
34. Yan Y, Wei H, Fu Y, Jusuf S, Zeng M, Ludwig R, Krystek SR Jr, Chen G, Tao L, Das TK (2016) Isomerization and oxidation in the complementarity-determining regions of a monoclonal antibody: a study of the modification-structure-function correlations by hydrogen-deuterium exchange mass spectrometry. *Anal Chem* 88(4):2041–2050. <https://doi.org/10.1021/acs.analchem.5b02800>
35. Macek B, Forchhammer K, Hardouin J, Weber-Ban E, Grangeasse C, Mijakovic I (2019) Protein post-translational modifications in bacteria. *Nat Rev Microbiol* 17(11):651–664. <https://doi.org/10.1038/s41579-019-0243-0>

Publisher's Note Springer Nature remains neutral with regard to jurisdictional claims in published maps and institutional affiliations.